

Electronic Supplementary Information

New-phased VO₂ Micro/nanostructures: Investigation of Phase Transformation and Magnetic Property

Liang Liu,^[a] Feng Cao,^[c] Tao Yao,^[b] Yang Xu,^[a] Min Zhou,^[a] Bingyan Qu,^[a] Bikai Pan,^[a]
Changzheng Wu,^[a] Shiqiang Wei^[b] and Yi Xie^{*,[a]}

[a] Department of Nanomaterials and Nanochemistry, Hefei National Laboratory for Physical Sciences at Microscale, University of Science and Technology of China, Hefei, Anhui, 230026 (P.R. China)

[b] National Synchrotron Radiation Laboratory, University of Science & Technology of China, Hefei, Anhui 230029, P.R. China

[c] College of Chemistry, Jilin University, Changchun, Jilin 130012, P. R. China

S1. The characterization and crystallographic information for the new-phased VO₂(D)

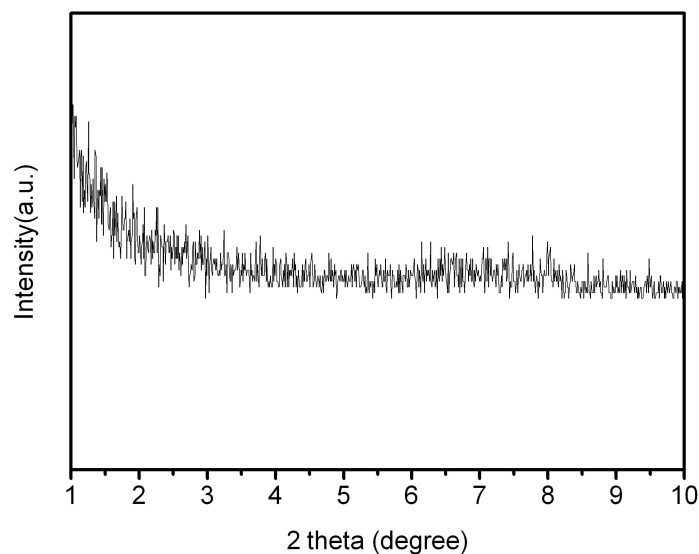


Figure S1. Low-angle XRD patterns of the new-phased VO₂(D) crystal structure.

Table S1. Crystallographic data and structural parameters obtained from X-ray powder diffraction.

compound name	vanadium dioxide (VO ₂)			
space group	P2/C (No. 13)			
Z	2			
crystal system	monoclinic			
lattice parameters	a = 4.5968 Å, b=5.6844 Å, c=4.9133 Å, β=89.39°			
cell volume	128.4 Å ³			
label	site	x	y	z
O(1)	4g	0.22	0.11	0.96
O(2)	4g	0.26	0.38	0.39
V(1)	2f	0.50	0.653	0.25
V(2)	2e	0.00	0.180	0.25

By using the crystal structure of monoclinic NiWO₄ as reference, we have calculated a new set of cell parameters (as shown in **Table S1**) for the new-phased VO₂(D). Also, we used monoclinic crystal geometry equation to achieve the theoretical d (Å) values based on the calculated cell parameters, which agrees well with the experimental d (Å) values of the new-phased VO₂(D) (as seen in Table S2 (ESI)).

Table S2. The summary information of the experimental and the theoretical d (Å) values calculated according to the crystallographic plane indices for the as-obtained new-phased VO₂(D).

(h k l)	theoretical d values (Å)	experimental d values (Å) *
100	4.5965	4.5968
011	3.7171	3.7172
110	3.5742	
111	2.9017	2.8961
020	2.8422	
002	2.4565	2.4566
120	2.4174	2.4248
200	2.2983	2.3009
121	2.1739	2.1670
210	2.1307	
211	1.9619	1.9627
022	1.8585	
202	1.6873	1.6778
20-2	1.6694	1.6757
13-1	1.6479	1.6414
21-2	1.6018	1.5805
222	1.4509	1.4460
23-1	1.3987	1.3719
140	1.3577	1.3538
213	1.3047	1.2942
004	1.2283	1.2264

* d-spacing of all the distinct visible peaks from the XRPD pattern

S2. The characterization of VO₂(B) in the absence of PVP in the reaction system

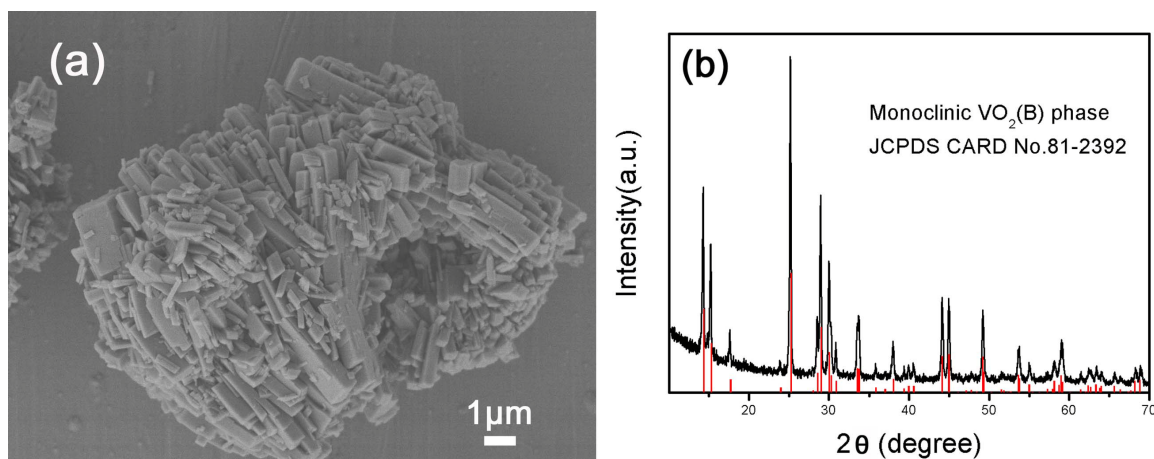


Figure S2. (a) XRD pattern and (b) FESEM images for the VO₂(B) in the absence of PVP in the reaction system.

Figure S2a shows a representative XRD pattern of the as-obtained VO₂(B) samples when no PVP in the reaction system. All the peaks can be perfectly indexed to the monoclinic VO₂(B) phase (JCPDS 81-2392) with lattice constants of $a=12.09 \text{ \AA}$, $b=3.702 \text{ \AA}$, $c=6.433 \text{ \AA}$, and $\beta=106.6^\circ$. Obviously, no peaks of any other phases were detected. **Figure S2b** shows the SEM image of typical sample composed of a very random aggregation, resulting in the final irregular morphology.

S3. The characterization of magnetic properties of the new-phased VO₂(D)

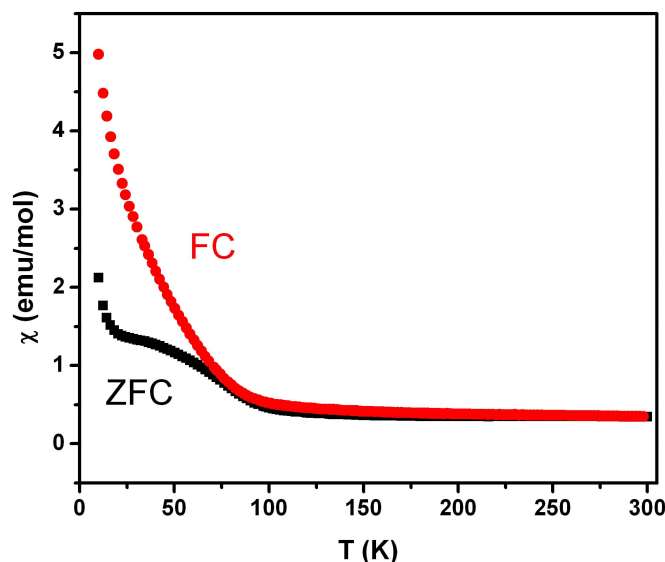


Figure S3. ZFC and FC magnetization measured as a function of temperature (4 to 300 K).

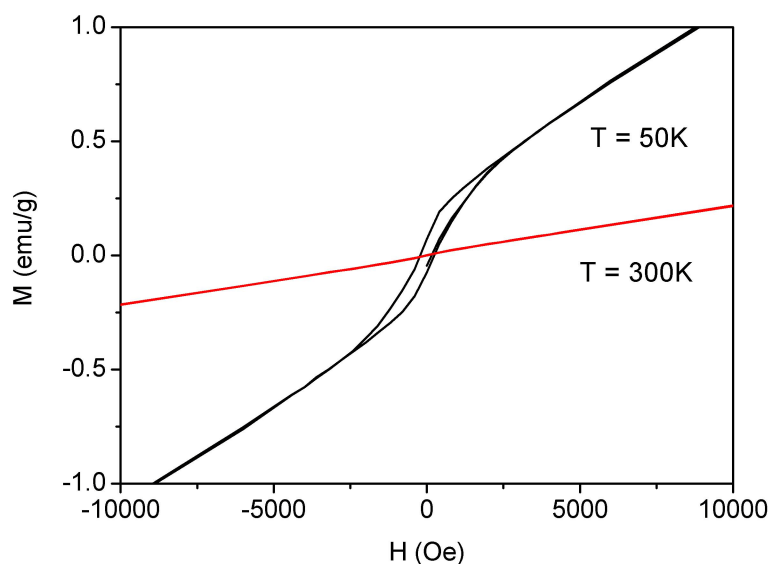


Figure S4. M – H curves of VO₂(D) at 50K and 300 K, respectively.

The existence of uncompensated spins in the system was further confirmed by M – H curves (**Figure S4**). M – H curves display a clear hysteresis at 2 K, which is an indication of weak ferromagnetism. However, the observation of the weak ferromagnetism can be attributed to the uncompensated spin in the system results a spin glass future.¹

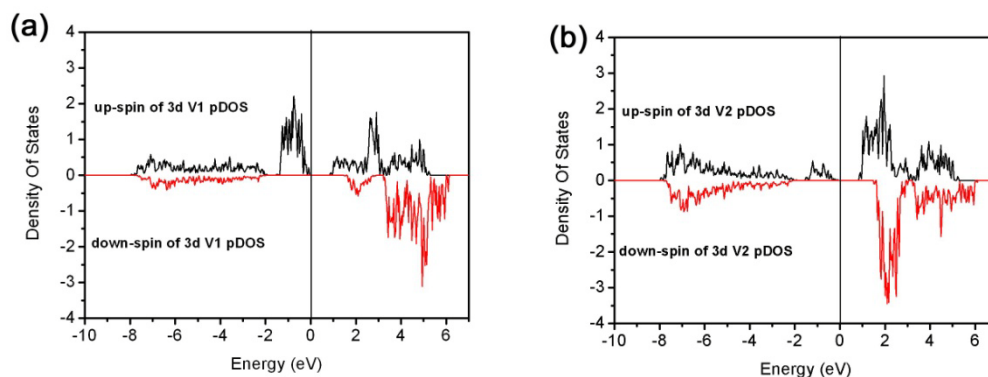


Figure S5. Calculated spin-resolved partial DOS of V(1)(a) and V(2)(b) 3d states of VO₂(D).

In VO₂, the magnetic moment is mainly localized on the V atom. To further investigate the nature of the magnetic properties, the spin-resolved DOS are computed by the tetrahedron method with Blöchl

corrections. **Figure S5a, b** shows the spin-resolved partial DOS of V(1) and V(2) atoms 3d orbitals separately.

We found there are two kinds of distorted octahedron ($[V(1)O_6]$ and $[V(2)O_6]$ respectively), which lead to the occurrence of magnetically nonequivalent vanadium sites in the structure. These vanadium sites can be presumably attributed to V^{4+} ($d1$, $S=1/2$) ions. $[VO_6]$ octahedra are coupled in edge-sharing $S=1/2$ antiferromagnetic zig-zag chains², which behave as spin-1/2 Heisenberg chains.

Then, we have performed Bader charge analysis³ on the V(1) and V(2) at spin-polarized levels. In the present studies, the charges per V atom is found to be very different, about 2.6957 $|e|$ for V(1) and 2.2394 $|e|$ for V(2), respectively. These results indicate that the different Coulomb interactions between V and the neighboring O atom at $[V(1)O_6]$ and $[V(2)O_6]$ octahedron. It is noted that the irregular octahedral distortion results in unequal charge distribution of the V atoms in the different $[VO_6]$ octahedral.

The magnetic moments calculated by integrating the spin densities over the Bader volume determined by the total charge densities from SIESTA GGA and VASP LDA calculations. These results showed that magnetic moment of $VO_2(D)$ with 1.6385 μ_B localized on V(1) and 0.3842 μ_B on V(2). Surprisingly, the magnetic moments at V(1) are around 4.26 times higher than that at V(2). From the discussion above, we conclude that the V(1) antiferromagnetic zigzag chains are surrounded by four nearly non-magnetic V(2) chains. The description is thus in terms of a one-dimensional Heisenberg system, which lead to such kind of susceptibility in **Figure S3**.

References:

1. HT Zhu, et al, Physica B: Condensed Matter, 2008, 403, 3141-3145.
2. E. Vavilova, et al, Physical Review B, 2006, 73, 144417.
3. R. Bader, Atoms in Molecules: A Quantum Theory, Oxford University Press, New York, 1990.